Studies of coronal mass ejections that have produced major geomagnetic storms

M. Mierla[1,2,3], D. Besliu-Ionescu[1,4], O. Chiricuta[1], C. Oprea[1], G. Maris[1]

[1] Institute of Geodynamics of the Romanian Academy, Bucharest, Romania

[2] Royal Observatory of Belgium, Brussels, Belgium

[3] Research Center for Atomic Physics and Astrophysics, Faculty of Physics, University of Bucharest, Romania

[4] CSPA, School of Mathematical Sciences, Clayton, Victoria, Australia

E-mail: marilena@geodin.ro

Accepted: 27 December 2009

Twenty five major geomagnetic storms (Dst < −150 nT) associated with clear coronal mass ejections (CMEs) at the Sun were produced in the period 1996 − 2008. There were 57 possible coronal mass ejections (CMEs) which could have produced these storms. We are studying these CMEs in order to see their propagation and possible interaction into the interplanetary space. We will also investigate possible connection between CMEs and solar seismic signatures. Their in-situ signatures and their correlation with geomagnetic indexes are also analyzed.

Coronal mass ejections; geomagnetic storms; solar quakes; CMEs kinematic analysis

Introduction

The analysis of coronal mass ejections (CMEs) which have produced major geomagnetic storms (geomagnetic index Dst < −150 nT) is a subject which was intensively studied in the past years (see e.g. Huttunen et al. 2002; Srivastava and Venkatakrishnan, 2004; Zhang et al. 2007; Echer et al. 2008; Gopalswamy et al. 2005, 2007, 2008; Gopalswamy 2008 etc.).

The main conclusions which were derived from the above mentioned studies are:

- The sources of the CMEs which produced major geomagnetic storms have a large spectrum: from less energetic (C-class) flares to very energetic (X-class) solar flares. Sometimes they are associated with prominence eruptions and sometimes, the sources of these CMEs are not visible on the solar disk (Huttunen et al. 2002).
- All these CMEs are halo CMEs (angular width around the occulter of the coronagraph bigger than 120 degrees). As a class, halo CMEs are more energetic than the rest of the CMEs and are associated with bigger soft X-ray flares (Gopalswamy et al. 2007).
- The vast majority of major storms arise from solar sources close to central meridian as seen from the Earth.
- The intensity of geomagnetic storms depends most strongly on the southward component of the interplanetary magnetic field (Bz), followed by the initial speed of the CME and the RAM pressure (Srivastava and Venkatakrishnan, 2004).

In this paper we are studying the CMEs in the period 1996-2008 which have produced major geomagnetic storms. Source regions are analyzed in an attempt to find possible connections between CMEs and solar seismic signatures. The speed of CMEs are compared with the ones recorded at ACE (close to the Earth) in order to infer possible interactions into the interplanetary space.

Data description

Twenty-five major geomagnetic storms (Dst < −150 nT) were registered in the period 1996 − 2008. Each of these storms was associated with interplanetary coronal mass ejections (ICMEs) observed by ACE spacecraft at L1 Lagrangian point.

An ICME is defined as a transient structure observed in situ which posses a combination of physical properties or signatures (e.g. magnetic field rotation, density decrease, electron temperature decrease etc. − see Zurbuchen and Richardson 2006). Very few ICMEs events, if any, possess all possible signatures together and usually some three signatures are required to identify an ICME (Jian et al. 2006). In general, the whole disturbance which defines an ICME comprises: the shock (if existing), the sheath, solar wind pile-up or compression region, "driver" or ejecta, plus ejecta wake or CME legs (see e.g. Rouillard 2011). Magnetic clouds (MC) are a particular class of ICMEs; they are ejecta associated with a smooth rotation of the magnetic field, a low plasma beta and low temperature (Burlaga et al. 1982; Forsyth et al. 2001).

To find the solar sources of these 25 ICMEs we checked solar images from SOHO in a time interval of up to 5 days previous each ICME was registered at ACE. We found a total of 57 halo CMEs which were directed towards the Earth and which could have been associated with the in-situ ICMEs signatures. It is possible that some of these events interact into the interplanetary space and arrive at ACE as a complex event. Also, the interaction with the

ambient solar wind may accelerate or decelerate these CMEs. Unfortunately, the gap of observations between the Sun and the Earth, does not allow us to observe directly these interactions. As a consequence, our analysis is based on some assumptions, which, nevertheless, take into account the solar and the in-situ signatures. One assumption is that all the CMEs directed towards the Earth which left the Sun one to five days before they actually arrived at ACE spacecraft, interacted into the interplanetary medium and arrived at the Earth as a complex event.

The data were divided into three parts:

The solar signatures comprises the 57 CMEs with: the observation time (format dd.mm.yyyy hh:mm) of first appearance in LASCO-C2 field of view; the source region type (X-ray flare class, prominence); source region location on the solar disc (latitude, longitude) as taken from http://solarmonitor.org/, the projected speeds etc. The projected speeds of the CMEs were taken from the LASCO CME catalog: http://cdaw.gsfc.nasa.gov/CME_list/. The speeds were calculated by fitting a second order polynomial function to the projected height-time diagram. The last measured speed in the field of view of LASCO-C3 was considered for our analysis.

In-situ signatures comprises the 25 ICMEs with: date and time of the disturbance, start and end time of the ejecta as taken from the ICME catalog: http://www.ssg.sr.unh.edu/mag/ace/ACElists/ICMEtable.html; speeds, magnetic field (B and Bz), plasma temperature, density.

Geomagnetic signatures comprises the 25 major geomagnetic storms with: the index Dst – its minimum value during the geomagnetic storm, date and time when this value was registered.

In-situ and geomagnetic parameters are provided by omni website: http://omniweb.gsfc.nasa.gov/form/dx1.html

Data Analysis

Our data set extends over the solar cycle 23 (SC 23) which started in June 1996 and ended in December 2008. The minimum phases of the SC 23 (average monthly sunspot number smaller than 20) are from June 1996 to May 1997 and from February 2006 to December 2008. It is observed that no one of our events happened at minimum of solar activity (the first event is observed in 1998 and the last one in 2005). Fig. 1 shows the number of storms versus time and over-plotted on it the monthly sunspot number of SC 23.

CME spherical model

In general, the speeds we measure in LASCO images are projected speeds. From one view direction only, is difficult to infer the real speeds, unless some assumptions are employed. In this study we assume that the CME is a sphere which propagates self-similar into the interplanetary space (Srivastava et al. 2009). This means that the radial speed is proportional with the expansion speed. The constant of proportionality is given by the tangent of the half angular width (*AW*) of the CME. All our CMEs are halo CMEs and as a consequence it is difficult to measure the angular widths. We take for *AW* three values: 30°, 85°, and 150°. The values of 30° and 150° are the minimum and maximum angular widths found by Cremades and Bothmer (2004) for a set of 120 limb CMEs, for which the angular widths could be measured. The width of 85° is the average value found from the 120 CMEs.

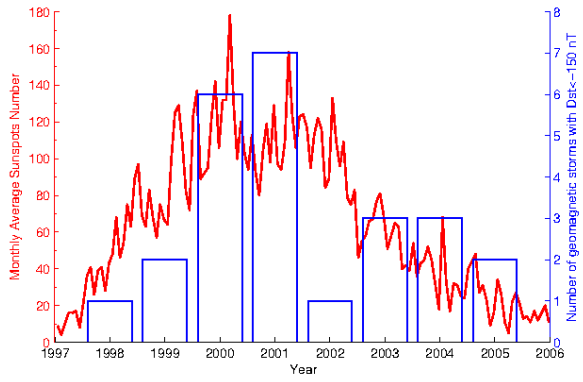

Fig.1. Number of geomagnetic storms per year (blue histograms) and monthly average sunspot number (red) versus time.

Fig. 2 shows the sketch of a spherical CME which propagates radially with a speed of V_{cent} and expands with a speed of V_{exp}. The speed towards the observer (V_{tt}) is derived from the equations:

$$V_{tt} = \left[V_{cent} \cdot \cos\alpha + \sqrt{V_{\exp}^2 - V_{cent}^2 \cdot \sin^2\alpha} \right] \cdot \cos\beta \quad (1)$$

$$V_{proj} \cdot \cos\beta = V_{cent} \cdot \sin\alpha + V_{\exp} \quad (2)$$

$$\frac{V_{\exp}}{V_{cent}} = \tan\left(\frac{AW}{2}\right) \quad (3)$$

where α and β are the latitude (absolute value) and the longitude in HEE (Heliocentric Earth Ecliptic) coordinate system (i.e. the X-axis is the Sun-Earth line, and Z-axis is the north pole for the ecliptic of date); *AW* is the angular width of the CME, V_{cent} is the radial speed, V_{exp} is the expansion speed and V_{proj} is the projected speed measured in LASCO images. In our case α varies from 0° to 28° and β from –47° to 95°.

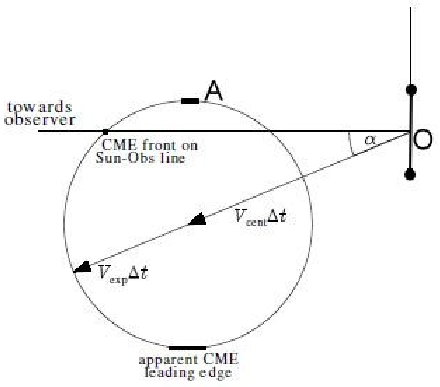

Fig. 2 A simple sketch of a spherical CME which expands self-similar. The center is assumed to propagate radially away from the Sun. The figure shows a meridional cut through the CME center. α is the propagation latitudinal angle. Adapted from Srivastava et al. (2009).

Travel time analysis

We derived the travel times of the CME from the Sun to the Earth calculated with different speed values as well as the real travel time. The real travel time (or shock travel time) is calculated as the difference between the time when the ICME disturbance (shock) arrived at the spacecraft and the time when the CME was observed in LASCO images. The travel time of a CME with a given speed V was calculated as the ratio between one astronomical unit (1 AU) and the speed V. For the speed V we used two different values: the projected speed of the CME (V_{proj}) and the calculated speed towards the observer (V_{tt}). Note, that in this way, we assume that the CME keeps a constant speed from the Sun to the Earth. The best correlation is observed to be between the real travel time and the travel time using V_{proj} (Fig. 3, upper panel).

A possible explanation for this is that the projected speed is a measure of the CME shock which propagates with the same speed in all the directions.

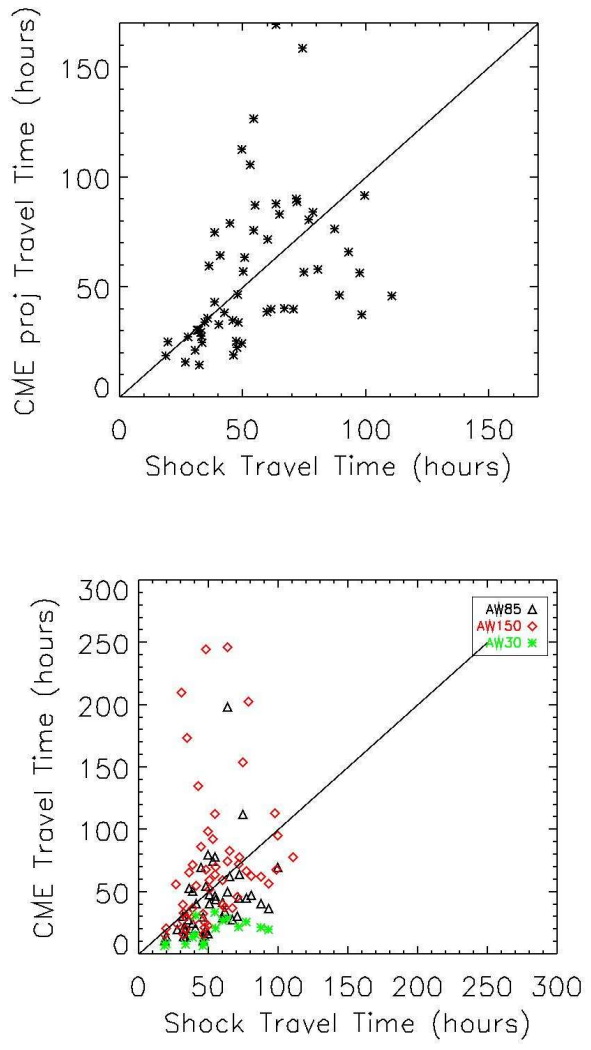

Fig. 3 Travel time of CMEs having a speed of V_{proj} (uper panel) and V_{tt} (lower panel) versus the real travel time. See text for more details.

For different angular widths of the CMEs, depending on the position of their source region on the disc, we calculate if the CMEs should arrive to the Earth or not. We plot only those CMEs which arrived at the Earth, according with our calculation (red rhombs are the CMEs with AW of 150° which arrived at Earth, black triangles: AW=85° and green stars: AW=30°) (Fig. 3, lower panel). We observe that very few CMEs with small angular widths arrived to the Earth. All the CMEs with AW of 150° arrived to the Earth, but in the same time, some of these CMEs have very small speeds compared with the ICME speeds registered at ACE. This is in the agreement with the fact that large CMEs are more influenced by the surrounding solar wind through the drag forces (see e.g. Manoharan and Rahman, 2011).

ICME parameters versus Dst

We calculated the correlation coefficient between the Dst index and the ICME parameters (Bz, speed, density, temperature) measured at the same time and one, two and three hours before the minimum Dst. The correlation coefficients between the Dst and the speed, temperature and density, respectively, were very small (smaller than 0.2). The best correlation coefficient was obtained between Dst and Bz measured two hours before minimum Dst (correlation coefficient of 0.76).

CMEs and solar quakes

Even if all our events have produced major geomagnetic storms (Dst < −150 nT), only three out of 57 CMEs were associated with solar quakes (Donea and Lindsey, 2005).

The one on 10 April 2001 was accompanied by proton event. The position of the sun quake was in the penumbra of the main spot. It was a two kernel structure with area about 32 Mm^2. This event was associated with a X2.3 class solar flare. The same region was the source of the CME which on 11 April, 23:00 UT produced a major geomagnetic storm (Dst = −271 nT). Noticeable is that the same active region produced two more CMEs on 9 April 2001. The active region was a complex one of Hale type: βγδ. The solar quake started 4 minutes before the X2.3 solar flare (at around 05:01 UT) and ended well before the peak of the flare (end of the quake: 05:09 UT, peak of the solar flare: 05:26 UT).

The 28 October 2003 sun quake was also associated with a proton event. A huge ribbon-like seismic emission was spreading away from the penumbra of the sunspot (NOAA AR 10486) to the western plages surrounding this sunspot. The same active region was the source of a X17.2 flare and the source of our CME which produced a major geomagnetic storm on 30 October 2003, 00:00 UT (Dst = −353 nT).

On 29 October 2003 a single compact signature spreading over 183 Mm^2 was observed, located in the eastern region of the penumbra, co-aligned with the magnetic neutral line. The event was also associate with a X10 solar flare. The associated geomagnetic storm was observed on 30 October 2003, 23:00 UT (Dst = −383 nT).

It is observed that the strongest two flares of our events are associated with solar quakes. Given the small number of events which were associated with solar quakes, we conclude that there is no association between the solar

quakes and the CMEs which produced major geomagnetic storms.

Discussion and conclusions

Twenty-five severe geomagnetic storms (Dst < −150 nT) where observed in the period 1996 − 2008 which were clearly associated with CMEs. 57 CMEs could have produced these storms.

We calculated the radial speeds of these CMEs using a spherical model which propagates self-similar (radial speed proportional with the expansion speed). We calculated the travel time of the CME using the component of the speed towards the observer obtained from the spherical model and the projected speed taken from LASCO CME catalog. We compared this with real travel time (calculated as the difference between the time when the ICME shock was observed at ACE and the time when the CME was first observed in LASCO-C2 field of view). Surprisingly, the best correlation was obtained with the projected speeds. This suggests that what we observe in LASCO images for halo CMEs are the shocks of these CMEs which propagates at the same speed in all directions. The scatter of these points compared with the diagonal in Fig. 3, shows the interaction of the CMEs with the ambient solar wind: some were decelerated and arrived at Earth later than predicted and some were accelerated and arrived at the Earth earlier than the actual travel time. This depend on the ambient solar wind speeds compared with the CMEs speeds. The same result was found by Gopalswamy et al. 2000, who inferred that in the interplanetary space the CMEs that are faster than the solar wind decelerate, while the CMEs that are slower than the solar wind accelerates to the speed of the wind.

The correlation of the ICME speed and Dst was small. The best correlation was found between the minimum Dst and Bz measured 2 hours before the minimum Dst. A very small correlation was found between the Dst index and other ICME parameters: speed, density, temperature.

Only three out of 57 CMEs were associated with solar quakes, implying that there is no visible correlation between the sun quakes and the CMEs which produced major geomagnetic storms.

Outlook

We intend to measure the expansion speeds for all our events. In this way we eliminate the assumption with the self-similar expansion and we can calculate the radial speed and the speed towards the observer from the system of the 2 equations described above.

Where possible, we will use the UVCS data to derive the line-of-sight speeds. This will constrain the calculation of the real speed and will help us improve the model of the CME.

Acknowledgements

We acknowledge the use of SOHO, ACE and geomagnetic data. The work of M.M., D.B.I., O.C. and C.O. was supported from the project TE nr. 73/11.08.2010.

References

Burlaga, L.F., Klein, L., Sheeley, N.R., Jr., Michels, D.J., Howard, R.A., Koomen, M.J., Schwenn, R., Rosenbauer, H., 1982, GeoRL 9, 1317.

Cremades, H., Bothmer, V., 2004, A&A 422, 307.

Donea, A.-C., Lindsey, C., 2005, ApJ 630, 1168.

Echer, E., Gonzalez, W.D., Tsurutani, B. T., Gonzalez, A.L.C., 2008, JGR 113, CiteID A05221.

Forsyth, R.J., Rees, A., Balogh, A., Smith, E.J., 2001, SSRv 97, 217.

Gopalswamy, N., Lara, A., Lepping, R.P., Kaiser, M.L., Berdichevsky, D., St. Cyr, O.C., 2000, GeoRL 27, 145.

Gopalswamy, N., Yashiro, S., Michalek, G., Xie, H., Lepping, R.P., Howard, R.A., 2005, GeoRL 32, CiteID L12S09.

Gopalswamy, N., Yashiro, S., Akiyama, S., 2007, JGR 112, CiteID A06112.

Gopalswamy, N., Akiyama, S., Yashiro, S., Michalek, G., Lepping, R. P., 2008, JASTP 70, 245.

Gopalswamy, N., 2008, JASTP 70, 2078.

Huttunen, K.E.J., Koskinen, H.E.J., Schwenn, R., dal Lago, A., 2002, in A. Wilson (ed.), ESA SP-506, Vol. 1. Noordwijk, ESA Publications Division, ISBN 92-9092-816-6.

Jian, L., Russell, C. T., Luhmann, J. G., Skoug, R. M., 2006, SoPh 239, 393.

Manoharan, P. K., Mujiber Rahman, A., 2011, JASTP 73, 671.

Rouillard, A.P., 2011, JASTP 73, 1201.

Srivastava, N., Venkatakrishnan, P., 2004, JGR 109, CiteID A10103

Srivastava, N., Inhester, B., Mierla, M., Podlipnik, B., 2009, SoPh 259, 213.

Zurbuchen, Thomas H., Richardson, Ian G., 2006, SSRv 123, 31.

Zhang, J., Richardson, I. G., Webb, D. F., Gopalswamy, N., Huttunen, E., Kasper, J. C., Nitta, N. V., Poomvises, W., Thompson, B. J., Wu, C.-C., and 2 coauthors, 2007, JGR 112, CiteID A10102.